Letter

Absence of the anomalous Hall effect in planar Hall experiments

C. M. Wang [1,2,3,4,5] Z. Z. Du,[4,2,3,5] Hai-Zhou Lu,[4,2,3,5,*] and X. C. Xie[6,7,8]

[1]*Department of Physics, Shanghai Normal University, Shanghai 200234, China*
[2]*Quantum Science Center of Guangdong-Hong Kong-Macao Greater Bay Area (Guangdong), Shenzhen 518045, China*
[3]*Shenzhen Key Laboratory of Quantum Science and Engineering, Shenzhen 518055, China*
[4]*Shenzhen Institute for Quantum Science and Engineering and Department of Physics, Southern University of Science and Technology (SUSTech), Shenzhen 518055, China*
[5]*International Quantum Academy, Shenzhen 518048, China*
[6]*International Center for Quantum Materials, School of Physics, Peking University, Beijing 100871, China*
[7]*Institute for Nanoelectronic Devices and Quantum Computing, Fudan University, Shanghai 200433, China*
[8]*Hefei National Laboratory, Hefei 230088, China*

(Received 30 November 2022; revised 1 May 2023; accepted 1 September 2023; published 14 September 2023)

Recently, the planar Hall effect has attracted tremendous interest. In particular, an in-plane magnetization can induce an anomalous planar Hall effect with a $2\pi/3$ period for hexagon-warped energy bands. This effect is similar to the anomalous Hall effect resulting from an out-of-plane magnetization. However, this anomalous planar Hall effect is absent in the planar Hall experiments. Here, we explain its absence, by performing a calculation that includes not only the Berry curvature mechanism, as those in the previous theories, but also the disorder contributions. The conventional π-period planar Hall effect will occur if the mirror-reflection symmetry is broken, which buries the anomalous one. This is because the anomalous planar Hall effect is of the higher order with respect to the small $h/(E_F\tau)$, when compared to the conventional planar Hall effect, with E_F being the Fermi energy and τ the relaxation time. We show that an in-plane strain can enhance the anomalous Hall conductivity and changes the period from $2\pi/3$ to 2π. We propose a scheme to extract the hidden anomalous planar Hall conductivity from the experimental data. Our work will be helpful in detecting the anomalous planar Hall effect and could be generalized to understand mechanisms of the planar Hall effects in a wide range of materials.

DOI: 10.1103/PhysRevB.108.L121301

Introduction. In the planar Hall effect, an in-plane transverse voltage can be induced by coplanar electric and magnetic fields, irrelevant to the Lorentz force. It used to be expected only in ferromagnetic and antiferromagnetic materials [1–6], but recently, it has attracted much attention in nonmagnetic materials. So far, there are three mechanisms: (i) the conventional mechanism [7–11]; (ii) the chiral anomaly [12–20], which is excluded in two-dimensional (2D) as chirality is defined in odd dimensions; and (iii) the newly proposed mechanism, the anomalous planar Hall effect induced by an in-plane magnetization, such as in spin-orbit coupled 2D systems [21–24], atomic crystals [25,26], topological materials [27–34], and heterodimensional superlattice [35,36]. In the third mechanism, in-plane magnetization can be tuned by an in-plane external magnetic field without introducing the Lorentz force.

However, the anomalous planar Hall effect is still absent in the planar Hall measurements. For example, it has been theoretically suggested that the hexagonal warping in the band structure, such as on the surface of a topological insulator [27,28,33], could lead to a $2\pi/3$ period of the anomalous planar Hall effect. However, measurements in the topological insulators $Bi_{2-x}Sb_xTe_3$ [7], Sn-doped $Bi_{1.1}Sb_{0.9}Te_2S$ [37], and Bi_2Te_3 [38] all show only a π period, despite the observed strong warping of these materials [39–42].

In this Letter, we propose a theory to understand the absence of the anomalous planar Hall effect in the experiments. The anomalous planar Hall effect requires breaking of all mirror-reflection symmetries [27] in addition to time-reversal symmetry breaking. However, the breaking of the mirror-reflection symmetry may also induce the conventional planar Hall effect with considerably large values because it is inversely proportional to the impurity density in diffusive systems. As a result, the total planar Hall conductivity is nearly identical to the conventional one, thereby implying that the anomalous planar Hall effect is covered by the conventional planar Hall effect. To illustrate our explanation, we use the hexagon-warped (threefold rotational symmetric) 2D surfaces states in a topological insulator as an example and calculate the planar Hall conductivity in the presence of an in-plane magnetic field. We further extend the previous researches [27,28,33] on the anomalous planar Hall effect by including disorder in the analysis. Though the intrinsic conductivity has been computed for this system analytically, a proper inclusion of the disorder has been missing; thus this work fills the gap. Up to the first order of the warping, only the anomalous planar Hall effect contributes to the Hall conductivity. Both

*Corresponding author: luhz@sustech.edu.cn

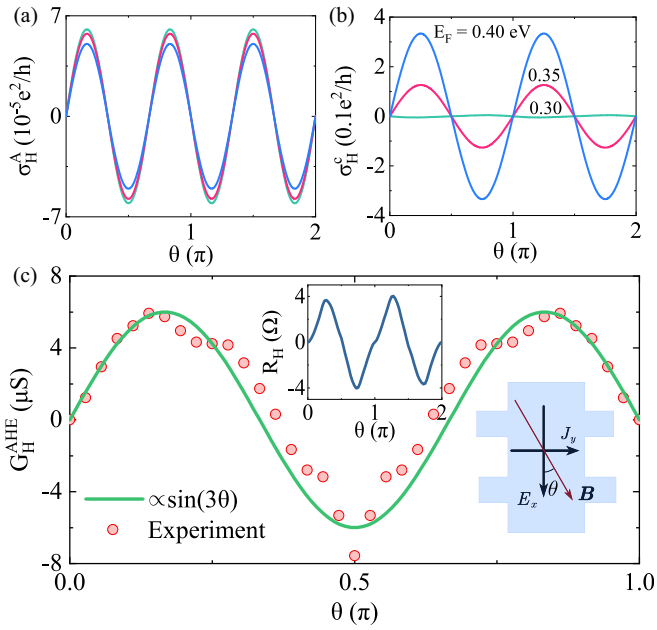

FIG. 1. [(a) and (b)] Comparison between the theoretically calculated anomalous planar Hall conductivity σ_H^A with a $2\pi/3$ period and conventional planar Hall conductivity σ_H^c with the π period. The parameters are $v = 0.3$ eV nm, $\alpha = 0.2$ eV nm^3, $\Delta = 0.01$ eV, $\tau = 2\hbar v^2/(n_i u_0^2 E_F) = 1$ ps, and $r = (n_i u_1^3)^{2/3}/(n_i u_0^2) = 0.1$. (c) The anomalous Hall conductance converted from the measured Hall resistance R_H (inset) and the longitudinal resistance R_{xx} in the experiment [37], as the difference (divided by 2) between the original Hall conductance data in the range of $\theta \in [0, 2\pi]$ and its mirror reflection with respect to $\theta = \pi$.

the intrinsic and noncrossing impurity-related extrinsic Hall conductivities are independent of the impurity density, except for the small higher-order skew-scattering contribution. They exhibit a $2\pi/3$ period [Fig. 1(a)] and a B^3 dependence on the in-plane magnetic field. Surprisingly, the conventional planar Hall effect occurs beyond the first order of the warping, with a B^2 dependence and a π period. Further, it is stronger than the anomalous planar Hall effect by several orders of magnitude [Fig. 1(b)]. These differences are listed in Table I. Hence, the total planar Hall conductivity has a π period, like those observed in the experiments. Because of the huge difference in magnitude, it is difficult to use the Fourier transformation to extract the anomalous planar Hall conductance from the experimental data. We propose to extract the anomalous planar Hall conductance as the difference (divided by 2) between two planar Hall conductance data sets. They are obtained by measuring the conductance as a function of the magnetic field angle $\theta \in [0, 2\pi]$ and its mirror reflection with respect to $\theta = \pi$. We apply this data analysis scheme to the experiment of the topological insulator Sn-doped $Bi_{1.1}Sb_{0.9}Te_2S$ [37]. It shows the extracted anomalous planar Hall conductance follows a $\sin(3\theta)$ dependence on the magnetic field angle with a $2\pi/3$ period [Fig. 1(c)]. Our work will be helpful for further investigations on the mechanisms of the planar Hall effects.

TABLE I. Comparison between the anomalous and conventional planar Hall effects, in the presence of the hexagonal warping with threefold rotational symmetry and in-plane strain at a relaxation time τ of about 1 ps. B is the in-plane magnetic field. The period is defined by θ in Fig. 1. e^2/h is the conductance quantum. Here θ is the angle between the magnetic and electric fields.

	Anomalous	Conventional
Magnitude	$10^{-5}\ e^2/h$	$10^{-1}\ e^2/h$
B dependence	B^3	B^2
Period (warping)	$2\pi/3$	π
Period (in-plane strain)	2π	π

Disorder-corrected planar Hall conductivity. Beyond the previous works [27,28,33] in which the Berry curvature is the only mechanism (intrinsic part), we also take into account the disorder contributions (extrinsic part) in the calculation of the anomalous planar Hall conductivity [43]. The intrinsic part is given by the summation of the z-component Berry curvature $\Omega_{z\boldsymbol{k}}^{\lambda}$ of the occupied states:

$$\sigma_H^{\text{in}} = \frac{e^2}{\hbar}\sum_{\lambda\boldsymbol{k}} \Omega_{z\boldsymbol{k}}^{\lambda} n_F(E_{\lambda\boldsymbol{k}}), \tag{1}$$

where n_F is the Fermi distribution at the λth band $E_{\lambda\boldsymbol{k}}$. The extrinsic part from the disorder scattering can be calculated [43] using the Feynman diagrams in Fig. 2.

We consider the hexagon-warped surface states of a topological insulator, in an in-plane magnetic field $\boldsymbol{B}$:

$$\hat{H} = v(k_x\sigma_y - k_y\sigma_x) + \frac{\alpha}{2}(k_+^3 + k_-^3)\sigma_z + \Delta_x\sigma_x + \Delta_y\sigma_y, \tag{2}$$

where v is the Dirac velocity; α measures the hexagonal warping that brings the threefold rotational symmetry; the in-plane magnetic field comes in terms of the Zeeman splitting $\boldsymbol{\Delta} = (\Delta_x, \Delta_y) = \Delta(\cos\theta, \sin\theta) = g\mu_B\boldsymbol{B}/2$, with g being the effective g factor; $\boldsymbol{\sigma} = (\sigma_x, \sigma_y, \sigma_z)$ are the Pauli matrices; and $k_\pm = k_x \pm ik_y$. The orbital contribution from the in-plane magnetic field relates to the z component of the vector potential, which will not enter into the two-dimensional Hamiltonian due to the Peierls substitution. Hence, there is no orbital contribution excluding the Lorentz force; thus, the planar Hall effect is purely induced by the in-plane magnetization due to the in-plane magnetic field. The warping term is the key to realize the anomalous planar Hall effect since the σ_z term is essential for the nonzero z-component Berry curvature. The warping coefficient could reach a considerable value up to 0.25eV nm^3 in the surface states of Bi_2Te_3-type topological insulators [39,41]. This model carries $\Omega_{z\boldsymbol{k}}^{\lambda} = \frac{\lambda v\alpha}{2\varepsilon_{\boldsymbol{k}}^3}[2vk_x(k_x^2 - 3k_y^2) + 3(\Delta_y k_x^2 + 2\Delta_x k_x k_y - \Delta_y k_y^2)]$, with $\lambda = \pm 1$. The expressions of eigenenergies including $\varepsilon_{\boldsymbol{k}}$ and velocities can be found in Ref. [43].

First, we study the intrinsic and noncrossing extrinsic contributions. Up to the first order of α, we find the anomalous planar Hall conductivity $\sigma_H \equiv \sigma_H^{\text{in}} + \sigma_H^{\text{ex}}$ as [43]

$$\sigma_H = \frac{e^2}{h}\left(\frac{4}{E_F} + \frac{u_1^3}{n_i u_0^4}\right)\frac{\alpha}{v^3}\Delta^3 \sin 3\theta, \tag{3}$$

where the third-order skew-scattering disorder correlations (the third and fourth diagrams in Fig. 2) result in the second term that is inversely proportional to the impurity density n_i. On the other hand, the intrinsic (Berry curvature) as well as the

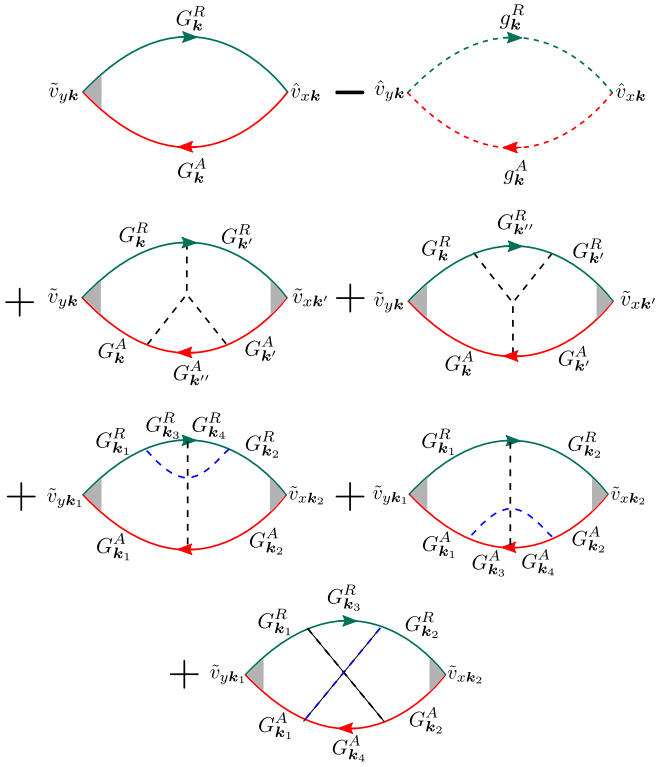

FIG. 2. The Feynman diagrams for the extrinsic contribution to the planar Hall conductivity. The arrowed solid and dashed lines stand for the full and bare Green's functions $G_{\boldsymbol{k}}^{R/A}$ and $g_{\boldsymbol{k}}^{R/A}$, respectively. The gray shadows represent the vertex correction to the velocity from the ladder diagrams. The dashed lines without arrows represent the disorder scattering. We model disorder as randomly located nonmagnetic δ-function impurities with the strength distributions satisfying $\langle u_i\rangle_{\rm imp}=0$, $\langle u_i^2\rangle_{\rm imp}=u_0^2$, and $\langle u_i^3\rangle_{\rm imp}=u_1^3$. The velocity $\hat{v}_\mu$ ($\mu=x$ and y) is corrected by disorder as $\tilde{v}_\mu(\boldsymbol{k})|_{k=k_F(\phi)}=\hat{v}_\mu(\boldsymbol{k})|_{k=k_F(\phi)}+n_i u_0^2\sum_{k'}G_{\boldsymbol{k}'}^A(E_F)\tilde{v}_\mu(\boldsymbol{k}')G_{\boldsymbol{k}'}^R(E_F)$, where n_i is the impurity density, and $k_F(\phi)$ is the Fermi wave vector, with ϕ being the polar angle.

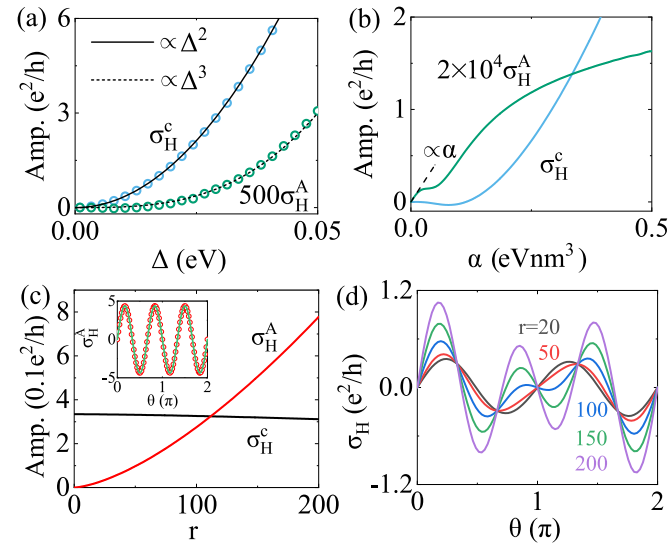

FIG. 3. The amplitudes of the anomalous and conventional Hall conductivities as functions of the Zeeman energy shown with circles (a), the warping coefficient α (b), and the dimensionless ratio $r=(n_i u_1^3)^{2/3}/n_i u_0^2$ that describes the third-order skew scattering (c). The inset of panel (c) shows the anomalous Hall conductivity for the weak warping coefficient $\alpha=0.001$ eV nm^3, where the circles are the numerical results while the green line is from Eq. (3). (d) The total Hall conductivities $\sigma_{\rm H}$ of different r are plotted as functions of the angle θ. The Fermi energy $E_F=0.4$ eV, the Fermi velocity $v=0.3$ eV nm, and $\tau=1$ ps. In panels (a) and (b), $r=0.1$. In panels (b)–(d), $\Delta=0.01$ eV. In panels (a), (c), and (d), $\alpha=0.2$ eV nm^3.

side-jump and other skew-scattering disorder contributions give rise to the first term that has nothing to do with n_i. Both terms $\propto B^3$ and show threefold rotational symmetry. The n_i-independent part is eight times the intrinsic (i.e., Berry curvature alone) planar Hall conductivity [33,43]. Up to the first order of α, the leading disorder contributions are fully due to the anomalous planar Hall effect and could strongly influence the intrinsic contribution. The term in the parentheses could be rewritten as $4/E_F+r^{1.5}\sqrt{E_F\tau/(2\hbar v^2)}$, with r being defined in Fig. 1. The parameter r determines the relative strength of the third-order skew-scattering contribution compared to other contributions.

Why are anomalous planar Hall effects much weaker than conventional planar Hall effects? Our theory can deal with the anomalous and conventional planar Hall effects in a unified way that fully takes into account the higher-order warping terms. We achieve this by numerical calculation with realistic sample parameters. The inset of Fig. 3(c) shows that the numerical $\sigma_{\rm H}^{\rm A}$ (the circles) at a weak warping $\alpha=0.001$ eV nm^3 agrees well with the analytical Eq. (3). This comparison confirms the accuracy of the numerical calculation. Beyond the weak warping limit, the mirror-reflection symmetry breaking will also result in a large conventional Hall conductivity inversely proportional to the impurity density. It is in vivid contrast to the out-of-plane magnetization case, where only the anomalous Hall effect exists [44]. The total planar Hall conductivity, which is the sum of $\sigma_{\rm H}^{\rm A}$ (anomalous) and $\sigma_{\rm H}^{\rm c}$ (conventional) in Figs. 1(a) and 1(b), exhibits approximately the same $\sin 2\theta$ behavior with the periodicity π as $\sigma_{\rm H}^{\rm c}$ in Fig. 1(b). The conventional $\sigma_{\rm H}^{\rm c}$ can be approximated by the classical Boltzmann one $\sigma_{\rm H}^{\rm Boltz}=-e^2\tau\sum_{\boldsymbol{k}}v_x v_y\delta(\varepsilon_{\boldsymbol{k}}-E_F)$ with the group velocities $v_{x,y}=\hbar^{-1}\partial_{k_{x,y}}\varepsilon_{\boldsymbol{k}}$. Up to the lowest order of the warping and the magnetic field,

$$\sigma_{\rm H}^{\rm Boltz}=\frac{e^2}{h}\frac{E_F\tau}{h}\frac{27\pi E_F^2}{4v^6}\Delta^2\alpha^2\sin 2\theta. \tag{4}$$

In the weak scattering regime ($\tau\sim$ ps), the dimensionless quantity $E_F\tau/h$ is very large, which in turn results in a significant disparity between the anomalous $\sigma_{\rm H}^{\rm A}$ and the conventional $\sigma_{\rm H}^{\rm c}$:

$$\sigma_{\rm H}^{\rm A}\sim\frac{e^2}{h}\frac{4\alpha}{v^3E_F}\Delta^3\ll\sigma_{\rm H}^{\rm c}\sim\sigma_{\rm H}^{\rm Boltz}. \tag{5}$$

Here the weak third-order impurity scattering term is ignored in $\sigma_{\rm H}^{\rm A}$. In summary, beyond the first order of warping, the conventional planar Hall conductivity exhibits a significantly larger value that obscures the anomalous one.

We can distinguish the small anomalous planar Hall effect from the conventional planar Hall effect, according

to their different magnetic field dependencies, as shown in Figs. 1(a) and 1(b). As expected, σ_H^A oscillates with a $2\pi/3$ period, while the period of σ_H^c is π. This π period originates from the conventional planar Hall part in σ_H^{ex} and $\propto 1/n_i$ as indicated by Eq. (4). The conventional planar Hall conductivity

$$\sigma_H^c(\boldsymbol{B}) = \sigma_H^c(-\boldsymbol{B}), \tag{6}$$

which has a $\sin 2\theta$ dependence. By contrast, the anomalous $\sigma_H^A \propto \sum_{\lambda \boldsymbol{k}} \Omega_z^\lambda$, where the Berry curvature is antisymmetrical $\Omega_z^\lambda(-\boldsymbol{B}, -\boldsymbol{k}) = -\Omega_z^\lambda(\boldsymbol{B}, \boldsymbol{k})$; then

$$\sigma_H^A(\boldsymbol{B}) = -\sigma_H^A(-\boldsymbol{B}). \tag{7}$$

This means the anomalous part is an odd function of the in-plane magnetic field. The amplitudes of σ_H^A and σ_H^c versus the Zeeman energy in Fig. 3(a) show the approximate relations $\sigma_H^A \propto \Delta^3$ and $\sigma_H^c \propto \Delta^2$, which verify the argument in Eqs. (6) and (7).

Dependence on Fermi energy and warping. For a small r (defined in Fig. 1), the amplitude of the anomalous planar Hall conductivity decreases with the increasing Fermi energy, roughly following $1/E_F$ as shown in Fig. 1. This behavior is in agreement with Eq. (3) and is in sharp contrast with the conventional planar Hall effect, whose amplitude is enhanced dramatically for $E_F > 0.3$ eV. Moreover, the amplitude of the conventional one does not vary with the increasing Fermi energy, monotonously. At the energy $E_F \sim 0.30$ eV, the conductivity almost vanishes. This complicated behavior implies the subtlety of the planar Hall effects.

Figure 3(b) illustrates the amplitudes of σ_H^A and σ_H^c as functions of the warping coefficient α. Both the anomalous and the conventional planar Hall effects vanish in the limit $\alpha \to 0$, indicating the important role of the warping in the planar Hall effect. The amplitude of the anomalous planar Hall conductivity increases monotonously with α, obeying the linear relation at weak α in the analytical Eq. (3), while it tends to saturate in the large-warping limit. For small warping, σ_H^c increases very slowly from zero and even shows a small and negative dip near $\alpha = 0.1$ eV nm^3; therefore, the total planar Hall conductivity equation (3) includes only the anomalous contribution up to the first order of α. Nevertheless, the amplitude of σ_H^c grows rapidly at large α. It is worth noting that we do not assume any anisotropic scattering or tilted energy band, which differs from previous works [7,9,10].

Enhanced anomalous planar Hall effect. The missing anomalous planar Hall conductivity could be found if the third-order skew scattering were larger. This is because the conventional one $\sigma_H^c \sim \sigma_H^{Boltz}$ is almost independent of r, while the third-order skew anomalous one is proportional to $r^{1.5}$. As revealed in Fig. 3(c), the amplitude of the anomalous part exceeds the conventional part when $r \approx 100$. Thus, the period of the total Hall conductivity shows a clear transition from π to $2\pi/3$ with increasing the r. The anomalous planar Hall part arising from the third-order skew scattering dominates in the total conductivity at large ratio r. The third-order skew scattering is a non-Gaussian disorder correlation, which usually yields contributions smaller than those described by the pair correlators. In order to observe the anomalous planar Hall effect in experiments, we propose to use strain to enhance it. The Zeeman energy $\Delta \sim 0.003$ eV at $B = 10$ T if $g = 10$. Hence, because of its Δ^3 behavior, the anomalous planar Hall effect is much smaller than the conventional planar Hall effect. It is known that the strain in the x-y plane could induce a term $\beta k_x \sigma_z$ [22,45,46] that breaks the mirror-reflection symmetry and reduces the C_{3v} symmetry to C_{1v}, which will result in another anomalous contribution with a 2π period in the planar Hall conductivity. Hence, the total planar Hall conductivity can be written as $\sigma_H = \sigma_H^c + \sigma_H^{A1} + \sigma_H^{A2} = C \sin 2\theta + A_1 \sin\theta + A_2 \sin 3\theta$, with σ_H^{A1} and σ_H^{A2} being the anomalous planar Hall conductivities induced by the strain and threefold warping, respectively. As σ_H^{A1} linearly depends on the magnetic field, it may be comparable to σ_H^c, especially in low-mobility samples. Therefore, the period may change from π to 2π by decreasing τ as demonstrated in Fig. 4(a), where the $2\pi/3$ period still does not appear. We can extract their amplitudes from the conductivities at $\theta = \pi/4$, $\pi/2$, and $5\pi/4$ [43], respectively, as shown in Fig. 4(b), where σ_H^{A1} is out-of-phase relative to σ_H^c and σ_H^{A2}, and then $\sigma_H^{A1} \propto \Delta$, $\sigma_H^{A2} \propto \Delta^3$, and $\sigma_H^c \propto \Delta^2$, as expected.

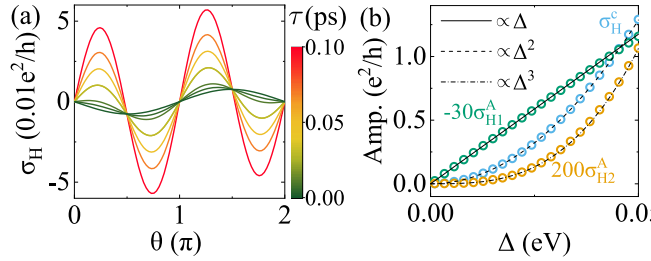

FIG. 4. (a) In the presence of an in-plane strain, the planar Hall conductivity σ_H at different relaxation times τ. (b) The amplitudes of the anomalous and conventional parts versus the magnetic field. The parameters are $E_F = 0.4$ eV, $v = 0.3$ eV nm, $\alpha = 0.2$ eV nm^3, $\beta = 0.1$ eV nm, $r = 0.1$, $\Delta = 0.01$ eV in panel (a), and $\tau = 0.1$ ps in panel (b).

The X and Ψ crossing diagrams (last three diagrams in Fig. 2) are well-known to play significant roles in the anomalous Hall effect [47,48]. We also consider their effects on the planar Hall effect and find that they lead to an anomalous planar Hall contribution [43], but with a π period instead of a $2\pi/3$ period. Nevertheless, its amplitude is 3 orders of magnitude smaller than that of the conventional planar Hall contribution. Therefore, our proposed data analysis scheme remains valid to distinguish the conventional and noncrossing anomalous planar Hall contributions, as long as the disorder scattering is weak. Furthermore, this scheme can distinguish the anomalous noncrossing and crossing contributions if the disorder scattering is strong.

Acknowledgments. We would like to thank Fengqi Song, Fucong Fei, Yoichi Ando, and Alexey Taskin for useful discussions. This work was supported by the National Key R&D Program of China (Grant No. 2022YFA1403700), the National Natural Science Foundation of China (Grants No. 11534001, No. 11974249, and No. 11925402), the Innovation Program for Quantum Science and Technology (Grant No. 2021ZD0302400), Guangdong province (Grants No.

2016ZT06D348 and No. 2020KCXTD001), the Natural Science Foundation of Shanghai (Grant No. 19ZR1437300), and the Science, Technology and Innovation Commission of Shenzhen Municipality (Grants No. ZDSYS20170303165926217, No. JCYJ20170412152620376, and No. KYTDPT20181011104202253). The numerical calculations were supported by the Center for Computational Science and Engineering of SUSTech.

[1] V. D. Ky, Planar Hall effect in ferromagnetic films, Phys. Status Solidi, b **26**, 565 (1968).
[2] H. X. Tang, R. K. Kawakami, D. D. Awschalom, and M. L. Roukes, Giant Planar Hall Effect in Epitaxial (Ga,Mn)As Devices, Phys. Rev. Lett. **90**, 107201 (2003).
[3] D. Y. Shin, S. J. Chung, S. Lee, X. Liu, and J. K. Furdyna, Temperature dependence of magnetic anisotropy in ferromagnetic (Ga,Mn)As films: Investigation by the planar Hall effect, Phys. Rev. B **76**, 035327 (2007).
[4] K. M. Seemann, F. Freimuth, H. Zhang, S. Blügel, Y. Mokrousov, D. E. Bürgler, and C. M. Schneider, Origin of the Planar Hall Effect in Nanocrystalline $Co_{60}Fe_{20}B_{20}$, Phys. Rev. Lett. **107**, 086603 (2011).
[5] W. N. Cao, J. Li, G. Chen, J. Zhu, C. R. Hu, and Y. Z. Wu, Temperature-dependent magnetic anisotropies in epitaxial Fe/CoO/MgO(001) system studied by the planar Hall effect, Appl. Phys. Lett. **98**, 262506 (2011).
[6] G. Yin, J.-X. Yu, Y. Liu, R. K. Lake, J. Zang, and K. L. Wang, Planar Hall Effect in Antiferromagnetic MnTe Thin Films, Phys. Rev. Lett. **122**, 106602 (2019).
[7] A. A. Taskin, H. F. Legg, F. Yang, S. Sasaki, Y. Kanai, K. Matsumoto, A. Rosch, and Y. Ando, Planar Hall effect from the surface of topological insulators, Nat. Commun. **8**, 1340 (2017).
[8] D. Huang, H. Nakamura, and H. Takagi, Planar Hall effect with sixfold oscillations in a Dirac antiperovskite, Phys. Rev. Res. **3**, 013268 (2021).
[9] S.-H. Zheng, H.-J. Duan, J.-K. Wang, J.-Y. Li, M.-X. Deng, and R.-Q. Wang, Origin of planar Hall effect on the surface of topological insulators: Tilt of Dirac cone by an in-plane magnetic field, Phys. Rev. B **101**, 041408(R) (2020).
[10] W. Rao, Y.-L. Zhou, Y.-j. Wu, H.-J. Duan, M.-X. Deng, and R.-Q. Wang, Theory for linear and nonlinear planar Hall effect in topological insulator thin films, Phys. Rev. B **103**, 155415 (2021).
[11] A. Yamada and Y. Fuseya, Negative magnetoresistance and sign change of the planar Hall effect due to the negative off-diagonal effective-mass in Weyl semimetals, Phys. Rev. B **105**, 205207 (2022).
[12] A. A. Burkov, Giant planar Hall effect in topological metals, Phys. Rev. B **96**, 041110(R) (2017).
[13] S. Nandy, G. Sharma, A. Taraphder, and S. Tewari, Chiral Anomaly as the Origin of the Planar Hall Effect in Weyl Semimetals, Phys. Rev. Lett. **119**, 176804 (2017).
[14] S. Nandy, A. Taraphder, and S. Tewari, Berry phase theory of planar Hall effect in topological insulators, Sci. Rep. **8**, 14983 (2018).
[15] M. Imran and S. Hershfield, Berry curvature force and Lorentz force comparison in the magnetotransport of Weyl semimetals, Phys. Rev. B **98**, 205139 (2018).
[16] D. Ma, H. Jiang, H. Liu, and X. C. Xie, Planar Hall effect in tilted Weyl semimetals, Phys. Rev. B **99**, 115121 (2019).
[17] A. Kundu, Z. B. Siu, H. Yang, and M. B. A. Jalil, Magnetotransport of Weyl semimetals with tilted Dirac cones, New J. Phys. **22**, 083081 (2020).
[18] G. Sharma, S. Nandy, and S. Tewari, Sign of longitudinal magnetoconductivity and the planar Hall effect in Weyl semimetals, Phys. Rev. B **102**, 205107 (2020).
[19] A. Ahmad and G. Sharma, Longitudinal magnetoconductance and the planar Hall effect in a lattice model of tilted Weyl fermions, Phys. Rev. B **103**, 115146 (2021).
[20] J. Ge, D. Ma, Y. Liu, H. Wang, Y. Li, J. Luo, T. Luo, Y. Xing, J. Yan, D. Mandrus *et al.*, Unconventional Hall effect induced by Berry curvature, Natl. Sci. Rev. **7**, 1879 (2020).
[21] Y. Zhang and C. Zhang, Quantized anomalous Hall insulator in a nanopatterned two-dimensional electron gas, Phys. Rev. B **84**, 085123 (2011).
[22] V. A. Zyuzin, In-plane Hall effect in two-dimensional helical electron systems, Phys. Rev. B **102**, 241105(R) (2020).
[23] J. H. Cullen, P. Bhalla, E. Marcellina, A. R. Hamilton, and D. Culcer, Generating a Topological Anomalous Hall Effect in a Nonmagnetic Conductor: An In-Plane Magnetic Field as a Direct Probe of the Berry Curvature, Phys. Rev. Lett. **126**, 256601 (2021).
[24] R. Battilomo, N. Scopigno, and C. Ortix, Anomalous planar Hall effect in two-dimensional trigonal crystals, Phys. Rev. Res. **3**, L012006 (2021).
[25] Y. Ren, J. Zeng, X. Deng, F. Yang, H. Pan, and Z. Qiao, Quantum anomalous Hall effect in atomic crystal layers from in-plane magnetization, Phys. Rev. B **94**, 085411 (2016).
[26] P. Zhong, Y. Ren, Y. Han, L. Zhang, and Z. Qiao, In-Plane Magnetization Induced Quantum Anomalous Hall Effect in Atomic Crystals of Group-V Elements, Phys. Rev. B **96**, 241103(R) (2017).
[27] X. Liu, H.-C. Hsu, and C.-X. Liu, In-Plane Magnetization-Induced Quantum Anomalous Hall Effect, Phys. Rev. Lett. **111**, 086802 (2013).
[28] R. S. Akzyanov and A. L. Rakhmanov, Surface charge conductivity of a topological insulator in a magnetic field: The effect of hexagonal warping, Phys. Rev. B **97**, 075421 (2018).
[29] Z. Liu, G. Zhao, B. Liu, Z. F. Wang, J. Yang, and F. Liu, Intrinsic Quantum Anomalous Hall Effect with In-Plane Magnetization: Searching Rule and Material Prediction, Phys. Rev. Lett. **121**, 246401 (2018).
[30] X. Guo, Z. Liu, B. Liu, Q. Li, and Z. Wang, Non-Collinear Orbital-induced Planar Quantum Anomalous Hall Effect, Nano Lett. **20**, 7606 (2020).
[31] H. Tan, Y. Liu, and B. Yan, Unconventional anomalous Hall effect from magnetization parallel to the electric field, Phys. Rev. B **103**, 214438 (2021).
[32] L. Jin, L. Wang, X. Zhang, Y. Liu, X. Dai, H. Gao, and G. Liu, Fully spin-polarized Weyl fermions and in/out-of-plane quantum anomalous Hall effects in a two-dimensional d0 ferromagnet, Nanoscale **13**, 5901 (2021).

[33] S. Sun, H. Weng, and X. Dai, Possible quantization and half-quantization in the anomalous Hall effect caused by in-plane magnetic field, Phys. Rev. B **106**, L241105 (2022).

[34] H. Wang, Y.-X. Huang, H. Liu, X. Feng, J. Zhu, W. Wu, C. Xiao, and S. A. Yang, Theory of intrinsic in-plane Hall effect, arXiv:2211.05978.

[35] J. Zhou, W. Zhang, Y.-C. Lin, J. Cao, Y. Zhou, W. Jiang, H. Du, B. Tang, J. Shi, B. Jiang *et al.*, Heterodimensional superlattice with in-plane anomalous Hall effect, Nature (London) **609**, 46 (2022).

[36] J. Cao, W. Jiang, X.-P. Li, D. Tu, J. Zhou, J. Zhou, and Y. Yao, In-Plane Anomalous Hall Effect in $\mathcal{PT}$-Symmetric Antiferromagnetic Materials, Phys. Rev. Lett. **130**, 166702 (2023).

[37] B. Wu, X.-C. Pan, W. Wu, F. Fei, B. Chen, Q. Liu, H. Bu, L. Cao, F. Song, and B. Wang, Oscillating planar Hall response in bulk crystal of topological insulator Sn doped $Bi_{1.1}Sb_{0.9}Te_2S$, Appl. Phys. Lett. **113**, 011902 (2018).

[38] A. Bhardwaj, S. Prasad P., K. V. Raman, and D. Suri, Observation of planar Hall effect in topological insulator—Bi_2Te_3, Appl. Phys. Lett. **118**, 241901 (2021).

[39] L. Fu, Hexagonal Warping Effects in the Surface States of the Topological Insulator Bi_2Te_3, Phys. Rev. Lett. **103**, 266801 (2009).

[40] M. Z. Hasan, H. Lin, and A. Bansil, Warping the cone on a topological insulator, Physics **2**, 108 (2009).

[41] Z. Alpichshev, J. G. Analytis, J.-H. Chu, I. R. Fisher, Y. L. Chen, Z. X. Shen, A. Fang, and A. Kapitulnik, STM Imaging of Electronic Waves on the Surface of Bi_2Te_3: Topologically Protected Surface States and Hexagonal Warping Effects, Phys. Rev. Lett. **104**, 016401 (2010).

[42] K. Kuroda, M. Arita, K. Miyamoto, M. Ye, J. Jiang, A. Kimura, E. E. Krasovskii, E. V. Chulkov, H. Iwasawa, T. Okuda *et al.*, Hexagonally Deformed Fermi Surface of the 3D Topological Insulator Bi_2Se_3, Phys. Rev. Lett. **105**, 076802 (2010).

[43] See Supplemental Material at http://link.aps.org/supplemental/10.1103/PhysRevB.108.L121301 for the detailed calculations.

[44] N. Nagaosa, J. Sinova, S. Onoda, A. H. MacDonald, and N. P. Ong, Anomalous Hall effect, Rev. Mod. Phys. **82**, 1539 (2010).

[45] S.-H. Zhang and B.-G. Liu, Anisotropic Rashba effect and charge and spin currents in monolayer BiTeI by controlling symmetry, Phys. Rev. B **100**, 165429 (2019).

[46] J. Kruthoff, J. de Boer, J. van Wezel, C. L. Kane, and R.-J. Slager, Topological Classification of Crystalline Insulators through Band Structure Combinatorics, Phys. Rev. X **7**, 041069 (2017).

[47] I. A. Ado, I. A. Dmitriev, P. M. Ostrovsky, and M. Titov, Anomalous Hall effect with massive Dirac fermions, Europhys. Lett. **111**, 37004 (2015).

[48] I. A. Ado, I. A. Dmitriev, P. M. Ostrovsky, and M. Titov, Anomalous Hall Effect in a 2D Rashba Ferromagnet, Phys. Rev. Lett. **117**, 046601 (2016).